Development of laser clads with high corrosion resistance for nuclear power industry

Cite as: AIP Conference Proceedings **2189**, 020011 (2019); https://doi.org/10.1063/1.5138623
Published Online: 22 November 2019

Pavla Bartoň Klufová, Antonín Kříž, and Marek Vostřák

Development of Laser Clads with High Corrosion Resistance for Nuclear Power Industry

Pavla Bartoň Klufová[1, a)], Antonín Kříž[1, b)] and Marek Vostřák[2, c)]

[1]*Department of Material Science and Technology, Faculty of Mechanical Engineering, University of West Bohemia, Univerzitní 22, 30100 Pilsen, Czech Republic*
[2]*New Technologies – Research Centre, University of West Bohemia, Univerzitní 8, 30100 Pilsen, Czech Republic*

[a)]Corresponding author: klufovap@fst.zcu.cz
[b)]kriz@kmm.zcu.cz
[c)]mvostrak@ntc.zcu.cz

Abstract. This contribution deals with development of a system consisting of a base material and a composite laser clad with high corrosion resistance. The cladding material for laser overlaying was a powder mixture of inorganic substances based on copper and oxides of silicon, iron, calcium and magnesium. Experiments were carried out with three types of powder mixtures with different copper-inorganic oxides ratios. The disk laser Trumpf TruDisk 8002 with wavelength λ=1030 nm was used for producing three laser clad specimens whose total area was 60×95 mm. The substrate was C45 steel. It was 20 mm in thickness and was ground on both sides. Structures of the composite clads were examined using light microscopy and scanning electron microscopy (SEM). Local chemical analysis of dendrites and interdendritic spaces was carried out using EDX in the SEM. The laser clads were found to possess very fine and unique microstructures. The corrosion resistance of the substrate-composite laser clads systems were assessed by means of an advanced electrochemical method of measuring the corrosion rate, which relied on potentiodynamic corrosion testing involving linear polarization. The corrosion resistance data was compared to results of conventional salt spray corrosion tests.

INTRODUCTION

Laser cladding relies on the high-energy-density laser beam to melt the base material as well as the cladding material. The latter may be in the form of powder or wire. The cladding process produces a narrow region, in which the melted cladding material and base material become metallurgically bonded. Their solidification thus leads to strong metallurgical bonds which provide the deposit with good cohesion as well as adhesion to the base material. The goal of laser cladding is to create a weld clad with desired properties and chemical composition on the base material without extensive dilution (>10%) between the two metals [1].

Laser cladding applications in the power generation and nuclear industries are not new. The first documented mention dates back to 1981 when a protective weld clad was deposited by laser on the joints between turbine blades and rotor in the Rolls Royce company [2]. Since then, advances in laser physics and materials engineering have expanded the range of laser cladding applications.

Among them, there is the unique concept of composite laser weld cladding for protection of outer surfaces of storage containers for spent nuclear fuel in underground repositories. In the Czech Republic, the fundamental requirements on storage containers have been set out by the State Office for Nuclear Safety (SÚJB). They include an extremely high corrosion resistance of the outer surface. The SÚJB stipulates that storage containers should retain their corrosion resistance for at least 100 000 years in the underground repository environment. The composite material for the corrosion-resistant outer layer of storage containers for spent nuclear fuel is based on materials and constituents that have existed on Earth since time immemorial. Degradation processes in chemically-pure metals

18th Conference of Power System Engineering, Thermodynamics and Fluid Mechanics
AIP Conf. Proc. 2189, 020011-1–020011-8; https://doi.org/10.1063/1.5138623
Published by AIP Publishing. 978-0-7354-1936-0/$30.00

(such as copper) and igneous rocks can be assessed reliably in order to obtain corrosion resistance predictions for the 100 000-year period defined by the SÚJB.

EXPERIMENTS

The purpose of the experimental programme was to contribute to development of a composite laser weld clad/base material with high corrosion resistance in a defined environment. The base material was C45 steel of 20 mm thickness ground on both sides. The chemical composition of C45 steel is shown in Table 1.

TABLE 1. Chemical composition of C45 steel, element content in weigh per cent [3]

	C	Si	Mn	Cr	P	S
C45 substrate	0.42 – 0.50	< 0.40	0.50 – 0.80	< 0.40	< 0.045	< 0.045

The cladding materials for laser deposition were mixtures of high-purity copper powder and inorganic substances based on complex oxides of silicon, iron, calcium and magnesium. The copper powder for laser cladding was supplied by Oerlicon Metco under brand name METCO 55. The chemical composition and specifications of the copper powder are listed in Table 2.

TABLE 2. Metco 55 powder; specifications and properties of powder as declared by the supplier [4]

	Copper content	Powder particle size	Morphology	Melting point	Density
METCO 55	Cu min. > 99%	45–90 μm	Spherical	1083°C	3–4 g/cm^3

Prior to laser cladding, METCO 55 was alloyed with a powder mixture of complex metal oxides. Table 3 gives the chemical composition of the oxide powder mixture, as determined by means of EDX analysis in a scanning electron microscope (SEM).

TABLE 3. Inorganic powder substances, EDX analysis of chemical composition, element content in weight per cent

	O	Mg	Al	Si	Ca	Ti	Cr	Ni	Mn	Fe	Cu
Inorganic powder substances	34.7	6.1	13.1	13.5	5.4	1.0	0.3	0.3	0.3	14.1	11.2

Three powder mixtures were prepared for experimental laser cladding. They had different ratios of copper and oxide powders:

- 95% Cu, 5% metal oxides,
- 90% Cu, 10% metal oxides,
- 85% Cu, 15% metal oxides.

Laser cladding was carried out at New Technologies Research Centre (NTC) at the University of West Bohemia. Solid-state disc laser Trumpf TruDisk 8002 was used. Its wavelength was $\lambda = 1030\ nm$ and the spot size was 3.4 mm. Weld cladding powder was supplied via powder feeder GTV PF 2/2 MH to coaxial-feeding cladding head Precitec YC52 with a four-beam nozzle. The assist and shielding gas was 99.99%-purity argon.

Two samples were prepared with each cladding powder mixture. There were six laser clad samples in total. Each laser clad sample had an area of 60×95 mm. Fig. 1 is a schematic illustration of the laser cladding process. It indicates three different regions of the laser clad: ZONE 1, ZONE 2 and ZONE 3:

- ZONE 1 – end of the first cladding track,
- ZONE 2 – centre of the laser cladding,
- ZONE 3 – beginning of the last cladding track.

Figure 2 shows macrographs of the laser-clad samples.

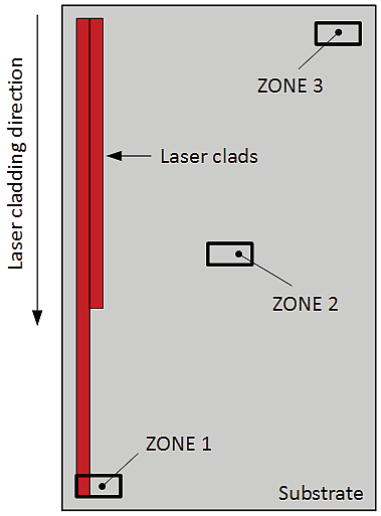

FIGURE 1: Schematic representation of the laser cladding process; ZONE 1, 2, and 3 are three different regions in a laser clad

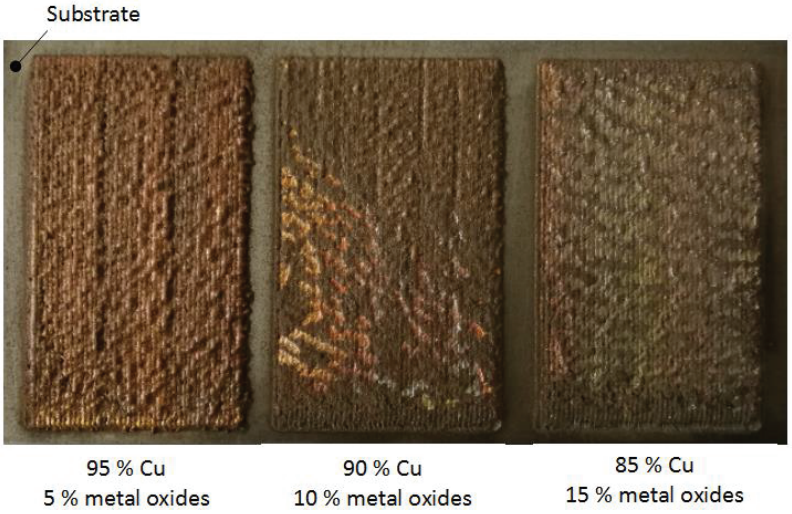

FIGURE 2: Macrographs of laser clad samples; copper and metal oxide ratios in cladding powders

METALLOGRAPHIC EXAMINATION

The laser clads were examined using metallographic techniques, Carl Zeiss Z1M light microscope with Axiovision software, and Philips XL 30 ESEM microscope with an EDX analyser. Their microstructures were revealed using a chemical mixture available under the name Robin. The interface between the laser clad and the base material was etched with 3 % nital.

In the course of metallographic preparation of '95 % Cu, 5 % metal oxides' specimen, the adhesion of the composite laser clad to the base material proved insufficient; and the clad separated from the substrate. For this reason, '95 % Cu, 5 % metal oxides' samples were disqualified from subsequent examinations.

OPTICAL MICROSCOPIC EXAMINATION OF SAMPLES

Laser clads are characterized by heterogeneous structure and chemical composition. Local variation of chemical composition occurs because the laser cladding process follows all the principles that govern fusion welding of dissimilar joints. Dilution between the clad and the base material occurs as the weld pool flows during solidification. The weld clad therefore absorbs elements from the base material. Insufficient dilution leads to macrosegregation regions, whose structure and properties differ from those of the weld clad matrix [5].

Figures 3, 4 and 5 show the structures of composite laser clads at 50 µm depth below the intended weld clad surface. The intended weld clad functional surface is produced by grinding, which removes excess material deposited by the cladding process. The purpose of taking micrographs at identical depths was to accurately capture the structural variations in the samples.

Figures 3 and 4 show micrographs of '90 % Cu, 10 % metal oxides' weld clad. Figure 3 is a micrograph of an epitaxial dendritic structure in ZONE 1. The interdendritic spaces in this very fine structure consist mostly of copper. Chemical composition variations between dendrites and interdendritic spaces are also indicated by the nature of the etch attack on the weld clad surface by the Robin reagent. Interdendritic spaces etch away, whereas dendrites remain intact.

Figure 4 is a micrograph of ZONE 2 in '90 % Cu, 10 % metal oxides' clad. The weld clad matrix consists mostly of copper and a dispersion of globular particles (their chemical analysis is reported in section below).

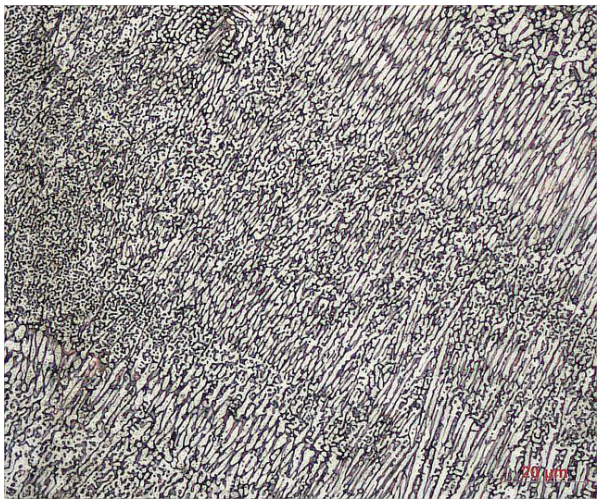

FIGURE 3: '90 % Cu, 10 % metal oxides'; ZONE 1; epitaxial dendritic structure, etched, magnification 1000×

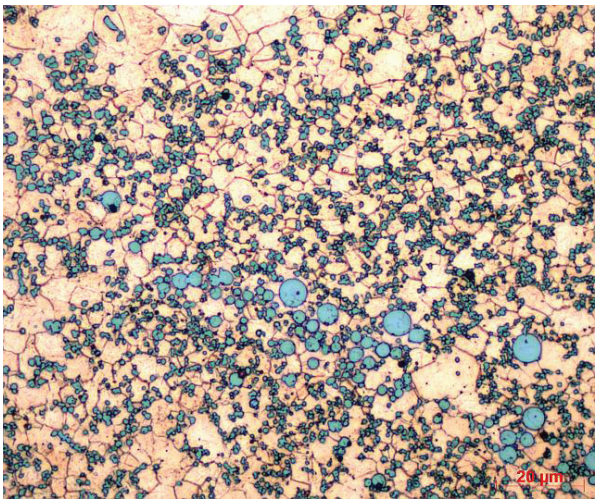

FIGURE 4: '90 % Cu, 10 % metal oxides'; ZONE 2; Cu-based matrix with dispersed particles, etched, magnification 1000×

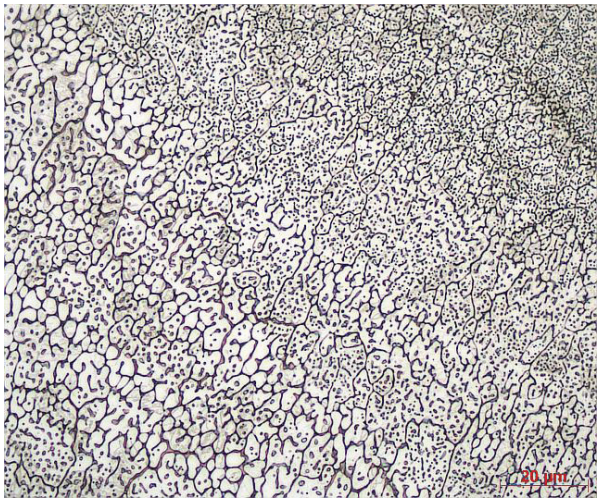

FIGURE 5: '85 % Cu, 15 % metal oxides'; ZONE 3; dendritic structure with notable interdendritic spaces consisting of copper; etched; magnification 1000×

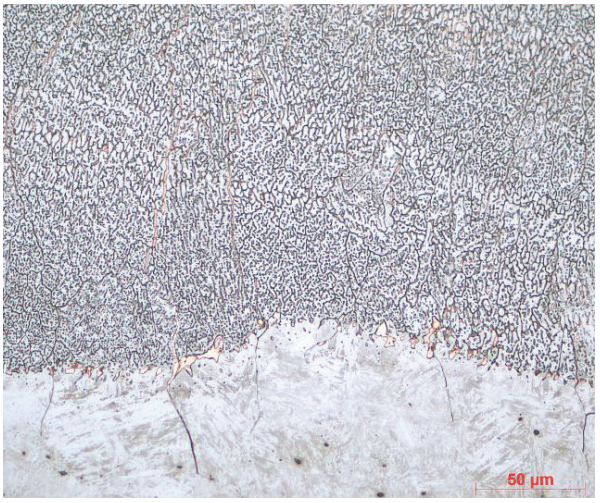

FIGURE 6: '85 % Cu, 15 % metal oxides'; ZONE 3; interface between the weld clad and the base material; cracks in the weld clad surface; etched; magnification 500×

Figure 5 is a micrograph of the dendritic structure in ZONE 3 in '85 % Cu, 15 % metal oxides' composite weld clad. In ZONE 3, which comprises the final laser cladding tracks, the growth of dendrites was found to have been affected by the heat supplied to the weld clad in making the previous tracks. Therefore the primary arms of the dendrites are longer than in Figure 3.

Figure 6 shows an interface between composite laser clad '85 % Cu, 15 % metal oxides' and the base material. Due to copper and iron immiscibility in solid state (as the binary diagram in Figure 7 indicates), a narrow interlayer forms at the fusion boundary once the surface of the base material becomes melted by the laser beam. This interlayer contains mostly copper. Figure 6 also shows cracks running from the base material surface to the core.

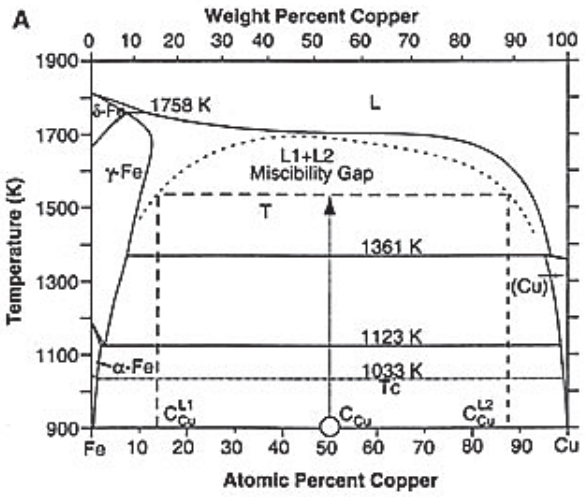

FIGURE 7: Fe-Cu binary diagram [6]

It is difficult to assess the microstructure of the composite laser clads using light microscopy. The reason is the very fine dendritic structure. At even the highest magnification available (1000×), it is impossible to reliably identify the phases present.

SCANNING ELECTRON MICROSCOPIC EXAMINATION OF SAMPLES

Scanning electron microscopy and EDX analysis of the samples were performed in order to identify particles of metal oxides and regions containing them. Differences in chemical compositions of main dendrite arms and interdendritic spaces were another aspect of interest. EDX measurements were taken in eight locations identified by the sequence EDX-M1 – EDX-M8 in Figures 8–11. Energy spectral information was collected using area (not point) measurement. The readings are given in Table 4.

TABLE 4. Inorganic powder substances, EDX analysis of chemical composition, element content in weight per cent

	Fe	Cu	Si	Mn	Ni	Ti	Cr	Ca	Al	Mg	O
EDX - M1	62.2	37.8	-	-	-	-	-	-	-	-	-
EDX - M2	14.1	11.2	13.5	0.3	0.3	1.0	0.3	5.4	13.1	6.1	34.7
EDX - M3	24.6	75.4	-	-	-	-	-	-	-	-	-
EDX - M4	72.9	26.8	0.3	-	-	-	-	-	-	-	-
EDX - M5	55.7	32.9	4.2	0.8	-	-	-	-	0.6	-	5.8
EDX - M6	62.8	37.2	-	-	-	-	-	-	-	-	-
EDX - M7	72.4	27.6	-	-	-	-	-	-	-	-	-
EDX - M8	30.9	69.1	-	-	-	-	-	-	-	-	-

Figure 8 is a micrograph of the dendritic microstructure in ZONE 1 of the '90 % Cu, 10 % metal oxides' weld clad. In location EDX-M1, the analysis covered the entire are of the image. The dendrites and interdendritic spaces were found to consist of 62.2 % Fe and 37.8 % Cu.

An undissolved metal oxide particle at the fusion boundary between the weld clad and the base material is shown in Figure 9. The measurement EDX-M2 (Table 4) identified it as one of inorganic oxide particles from the cladding powder. Figure 10 is a micrograph of the dendritic structure in 'Cu 85 %, metal oxides 15 %' weld clad. In this

region, chemical compositions were measured in an interdendritic space (EDX-M3) and in a dendrite arm (EDX-M4). As Table 4 shows, interdendritic spaces contain mostly copper, whereas iron dominates in dendrites.

Measurements in locations EDX-M5 through EDX-M8 were taken in ZONE 3 on '85 % Cu, 15 % metal oxides' sample. The interdendritic space identified in Figure 11 as EDX-M5 contains iron, copper, silicon, manganese, aluminium and oxygen bound in oxides. Measurements EDX-M6 through EDX-M8 only found iron and copper in various amounts, depending on the location.

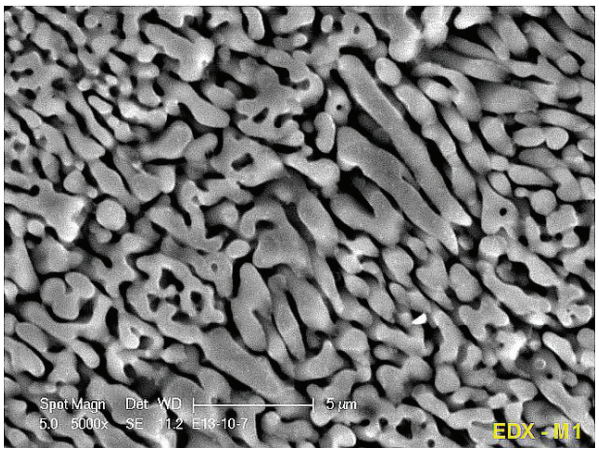

FIGURE 8: '90 % Cu, 10 % metal oxides'; ZONE 1; dendritic structure; etched; magnification 5000×

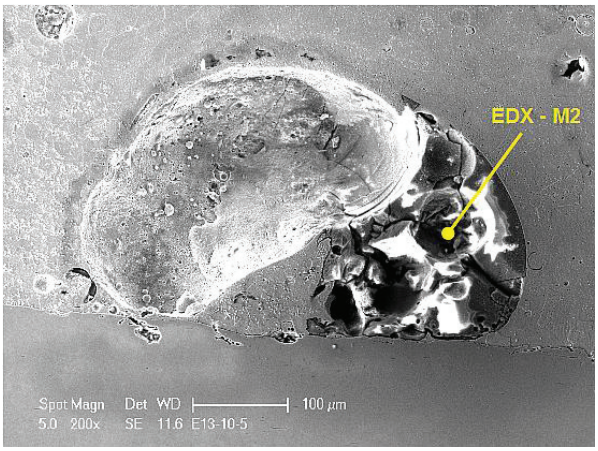

FIGURE 9: '90 % Cu, 10 % metal oxides'; ZONE 2; undissolved complex oxide at fusion boundary; etched; magnification 200×

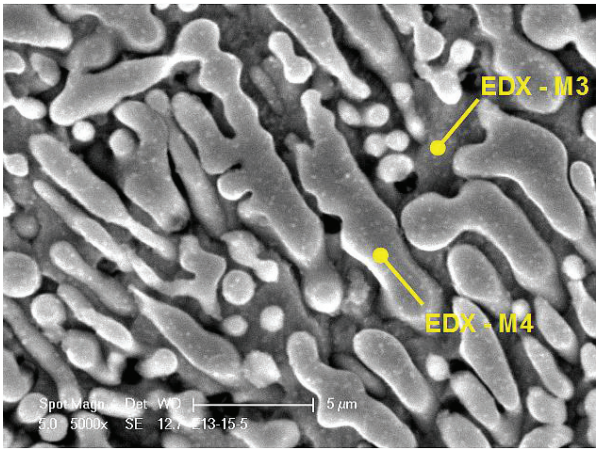

FIGURE 10: '85 % Cu, 15 % metal oxides'; ZONE 2; dendritic structure; etched; magnification 5000×

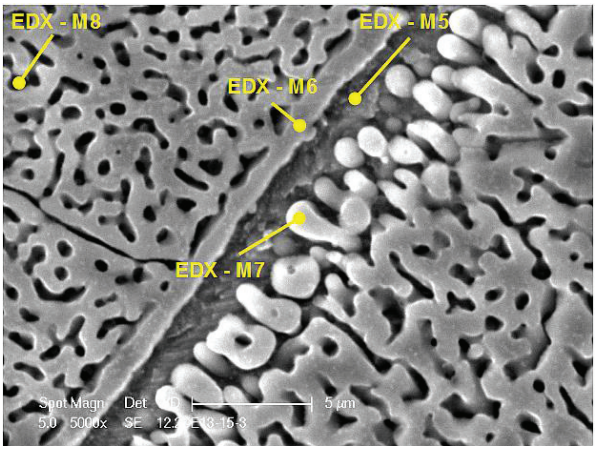

FIGURE 11: '85 % Cu, 15 % metal oxides'; ZONE 3; dendritic structure; etched; magnification 5000×

CORROSION RESISTANCE OF THE BASE MATERIAL-WELD CLAD SYSTEM

Corrosion resistance of the composite laser clads was assessed using potentiodynamic corrosion testing with the aid of BioLogic SP-150 potentiostat. EcLab 10.44 software was employed for data processing and evaluation. First, the time dependence was measured of the steady-state corrosion potential between *WE - WORKING ELECTRODE* and *RE - REFERENCE ELECTRODE*. The time for stabilization of free corrosion potential was identical in all measurements $t_R = 30$ min. The, linear polarization was used for finding the dependence of corrosion current (converted to current density) on the mixed corrosion potential of the sample within the range from E_i to E_L ($E_i = E_{corr} - 0{,}025\ [V]$; $E_i = E_{corr} + 0{,}025\ [V]$) with respect to the reference electrode (*RE*). The Tafel lines obtained

were extrapolated using software EcLab 10.44 and the polarisation resistance R_p *[mV]* and corrosion rate v_{corr} *[µm/year]* were determined [1].

The electrolyte used for measuring the corrosion resistance of the composite weld clad/base material system was artificial mine water. It was chosen in order to simulate the actual environment of underground repositories for storage containers.

The weld clads were prepared for measurement by grinding to the intended thickness in a magnetic grinding machine. Potentiodynamic corrosion testing involved three measurements on each laser clad sample. One measurement on a copper sheet of 99.98 % purity was used as the reference standard for comparing the measured and calculated corrosion rates. The corrosion rates obtained were converted to corrosion rates over a 100 000-year period (as stipulated by the SÚJB), assuming linear loss of laser clad and copper sheet with time.

The data from the potentiodynamic corrosion test are summarized in Table 5.

TABLE 5. Potentiodynamic corrosion test; measured and calculated steady-state corrosion potential, polarisation resistance and corrosion rate

Designation of sample	Number of measurements	Corrosion potential E_{corr} [mV vs RE]	Polarisation resistance R_p [Ω]	Polarisation resistance.S [Ω.cm^2]	Corrosion rate [µm/year]	Corrosion rate over 100 000 years [mm]
Cu sheet	1	-175	6334	11211	0.023	2
	1	-352	82499	146023	0.284	28.4
LC 90/10	2	-535	4670000	8265900	0.006	0.6
	3	-505	76917	136143	0.442	44.2
	1	-491	9270000	16407900	0.003	0.3
LC 85/15	2	-535	8120000	14372400	0.003	0.3
	3	-510	9870000	17469900	0.003	0.3

The measured corrosion rates for composite laser clads converted to corrosion rates over 100 000 years are almost one order of magnitude slower than those of the copper sheet reference standard. However, the heterogeneity, porosity, internal defects and cracks in laser clads, which form in the course of the complicated process of laser cladding with high-purity copper, dramatically reduce corrosion resistance (as illustrated in Figures 12 and 13).

Macrographs in Figures 12 and 13 show the surfaces of composite laser clads prior to salt spray corrosion tests and after 24-hour exposure.

90 % Cu, 10 % metal oxides

Before corrosion test | After 24-hour corrosion test

FIGURE 12: '90 % Cu, 10 % metal oxides'; surfaces of laser clads before and after salt spray corrosion testing

85 % Cu, 15 % metal oxides

Before corrosion test | After 24-hour corrosion test

FIGURE 13: '85 % Cu, 15 % metal oxides'; surfaces of laser clads before and after salt spray corrosion testing

CONCLUSION

Using laser cladding, six samples were prepared for experiments. The weld clad material was a mixture of high-purity copper powder (METCO 55) with additions of complex oxides of silicon, iron, calcium and magnesium in 5 %, 10 % and 15 % amounts. Samples of laser clads '90 % Cu, 10 % metal oxides' and '85 % Cu, 15 % metal oxides' were examined using light and scanning electron microscopes. Metallographic analysis revealed both chemical and structural heterogeneities of the laser clads. The corrosion resistance of the laser clads was assessed by potentiodynamic corrosion testing. The corrosion rates obtained were converted to corrosion rates over a 100 000-year period (assuming linear corrosion loss of laser clad with time). The corrosion rate of laser clad '85 % Cu, 15 % metal oxides' was 0.3 mm/100 000 years. A reference corrosion test in the form of the salt spray test was performed for comparison. Owing to severe porosity and internal defects in the laser clads, the samples were attacked within 24 hours of the salt spray test.

ACKNOWLEDGMENTS

The authors gratefully acknowledge the funding for these tests provided under the applied research project of the Technology Agency of the Czech Republic ZETA TJ01000316.

REFERENCES

1. P. Klufová, *Degradace laserem navařených austenitických vrstev*, Disertační práce, Západočeská univerzita v Plzni, 2018
2. I. Hemmati, *Laser-deposited metallic coatings,* Ph.D. Thesis, Zernike Institute: 2013-17, ISBN 978-90-77172-94-0
3. Přehled vlastností oceli C45, www.bolzano.cz [citation 27.4.2019]
4. Oerliko Metco, Datasheet – Metco 55, *https://www.oerlikon.com/* [citation 27.4.2019]
5. J. Liu, J. Li, X. Cheng, H. Wang, *Effect of dilution and macrosegregation on corrosion resistance of laser clad AerMet100 steel coating on 300M steel substrate,* In Surface & Coatings, Vol. 325. 2017, p. 352-359, ISSN 0257-8972
6. K. Uenishi et al., *Laser Cladding of Fe-Cu Based Alloys on Aluminum*, Solid State Phenomena, Vol. 127, pp. 331-336, 2007